



Piezoelectric detection of the photoacoustic signals of n-type GaAs single crystals

メタデータ	言語: eng 出版者: 公開日: 2020-06-21 キーワード (Ja): キーワード (En): 作成者: 碓, 哲雄, 福山, 敦彦, 横山, 宏有, 前田, 幸治, 二神, 光次, Miyazaki, K メールアドレス: 所属:
URL	<a href="http://hdl.handle.net/10458/5316">http://hdl.handle.net/10458/5316</a>

# Piezoelectric detection of the photoacoustic signals of *n*-type GaAs single crystals

T. Ikari, K. Miyazaki, A. Fukuyama, H. Yokoyama, K. Maeda, and K. Futagami  
*Department of Electronics, Miyazaki University, 1-1 Gakuenkibanadai, Miyazaki 889-21, Japan*

(Received 29 May 1991; accepted for publication 15 November 1991)

Piezoelectric photoacoustic (PA) measurements on liquid-encapsulated-Czochralski-grown *n*-GaAs were carried out at room temperature. A continuous broad band below 1.35 eV and a peak at 1.383 eV were observed in the PA amplitude spectra. By comparing with the optical-absorption spectra, it is concluded that the broad band is due to the electron transition involving the EL2 deep-lying defect levels. For the observed peak at 1.383 eV, the origin is considered to be dislocation related. The possibility that this peak is an apparent one expected from the proposed models for the PA signal generation is denied.

## I. INTRODUCTION

Photoacoustic (PA) measurements have recently been used to investigate physical properties of semiconductors.<sup>1</sup> One of the great advantages of a PA measurement is that it is a direct monitor of a nonradiative relaxation channel. Therefore, the PA technique may complement absorption and photoluminescence (PL) spectroscopic techniques. A piezoelectric PA measurement has been recently developed by Jackson and Amer<sup>2</sup> utilizing a piezoelectric transducer (PZT) as a PA signal detector. Since the transducer has a wide frequency response and can be used over a wide range of temperature and pressure, the transducer method becomes more useful for physical interest as well as industrial requirements.<sup>3</sup> By using the ZnO-sputtered film transducer, Wasa, Tsubouti, and Mikoshiba have succeeded in observing nonradiative deexcitation signals in the PA spectra of CdS by comparing with their PL spectra.<sup>4</sup>

Another advantage of PA measurements is that they are sensitive enough to measure the very small optical-absorption coefficient  $\beta$  in a highly transparent medium. Typical examples are investigations for the midgap states of amorphous semiconductors. Since the conventional absorption and reflection experiments cannot measure the absorption coefficient  $\beta$  smaller than about  $10 \text{ cm}^{-1}$ , the localized states removed from the Urbach's tail of amorphous semiconductors are usually difficult to observe optically. However, using PA spectroscopy, Caesar, Abkowitz, and Lin detected low values of  $\beta$  as low as  $10^{-1} \text{ cm}^{-1}$  for the amorphous Se thin films with thicknesses less than  $20 \mu\text{m}$ .<sup>5</sup> This fact indicates that the PA technique should be quite useful in detecting low-optical-absorption coefficients in such thin-film samples.

The two advantages discussed above indicate that the PA measurements will be a useful tool for investigating the deep-lying defect levels in GaAs such as EL2. These levels usually involve nonradiative electron transitions due to the strong electron-lattice interaction and their concentration is very low, e.g., of the order of  $10^{16} \text{ cm}^{-3}$  for the EL2. We have already reported the preliminary results of the PA spectra of GaAs single crystals below room temperature,<sup>6</sup> and we have considered that the observed peak below the energy gap  $E_g$  is related to the dislocation densities. How-

ever, the possibility that the observed peak is an apparent one has still remained. In this paper, we extensively discuss the origin of the peak by adding further experimental results and by taking into account the calculated spectra using proposed models for the PA signal generation mechanism.

## II. EXPERIMENTAL PROCEDURES AND RESULTS

The samples were cut from an unintentionally doped *n*-type GaAs wafer grown by the liquid-encapsulated-Czochralski (LEC) method. The resistivity was of the order of  $10^6 \Omega \text{ cm}$ . The typical sample dimensions were  $0.5 \times 0.5 \times 0.05 \text{ cm}^3$ . The PZT detector was attached to the rear surface of the sample with respect to the incident light using a silver conducting paste to obtain good thermal and mechanical contacts. The incident light from the grating monochromator was mechanically chopped at frequencies ranging from 77 to 860 Hz. The experimental configurations of the sample and the detector have been reported in detail previously.<sup>3,7</sup> Since the resonant frequency of the PZT was 193 kHz, our experiments were carried out in off-resonant conditions. The pellets cut from the wafer were polished and lapped by using an alumina powder (particle size of  $0.3 \mu\text{m}$ ) to obtain thin samples for the measurements of the sample thickness dependence of the PA spectra. The chemical etching to obtain a mirrorlike surface was carried out by immersing the sample in a  $\text{H}_2\text{SO}_4(3):\text{H}_2\text{O}_2(1):\text{H}_2\text{O}(1)$  solution and the etching rate was  $40 \mu\text{m}/\text{min}$ .

The photoacoustic (PA) amplitude and the phase spectra of *n*-GaAs at room temperature are shown in Figs. 1(a) and 1(b), respectively, where the modulation frequency  $f$  was varied from 77 to 800 Hz. The thickness of the sample was  $530 \mu\text{m}$ . The actually observed PA signal voltages are of the order of a few tens of microvolts, and are indicated in the ordinate. The PA amplitude signal increases gradually with the incident photon energy  $h\nu$  and has a distinctive peak at 1.383 eV followed by a dip at 1.40 eV. Hereafter, we refer to this peak as the A peak. Above the  $h\nu$  of 1.40 eV, the amplitude signal rises steeply up to 1.42 eV and changes its slope more gradually. The energy of this edge agrees well with the energy gap  $E_g$  of GaAs,

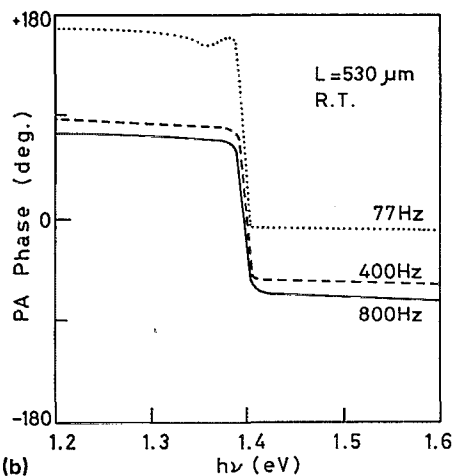
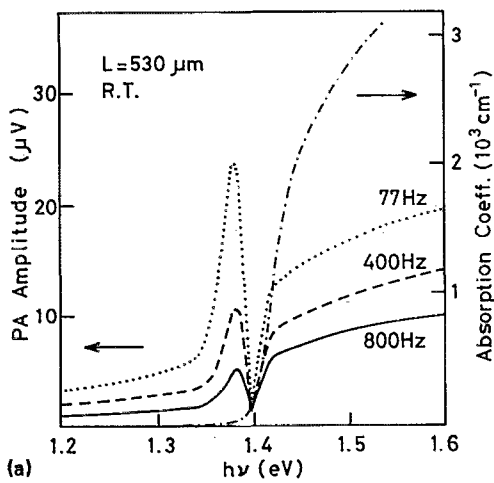


FIG. 1. (a) The photoacoustic (PA) amplitude and (b) the phase spectra of *n*-GaAs at room temperature where  $f = 77$  Hz (dotted), 400 Hz (dashed), and 800 Hz (solid curve), and  $L = 530 \mu\text{m}$ . The absorption spectra at room temperature are also shown by the dot-dashed curve in the amplitude spectra.

1.42 eV, at room temperature. When the modulation frequency increases, the height of the A peak decreases as  $f^{-0.7}$ ; however, the height above  $E_g$  decreases more gradually as  $f^{-0.5}$ . Similar PA amplitude spectra have also been observed for semi-insulating (SI) GaAs.<sup>6</sup>

The PA phase signal at  $f = 77$  Hz remains constant below about 1.38 eV except a small dip near 1.36 eV as shown in Fig. 1(b). Just above the energy of 1.38 eV, near the A peak in the amplitude spectra, the phase is drastically delayed by 180°. No phase shift was observed by the further increase of  $h\nu$  above  $E_g$ . When the modulation frequency increases, the overall features for the PA phase spectra are unchanged. However, the rigid shift of the phase to the lower values is observed and the dip near 1.36 eV smears out.

Figures 2(a) and 2(b) show the PA amplitude and the phase spectra, respectively, for the samples of different thickness  $L$  at room temperature. The modulation frequency was set at 77 Hz. The PA amplitude and the phase spectra for the 277- $\mu\text{m}$ -thick sample [dashed curve in Fig.

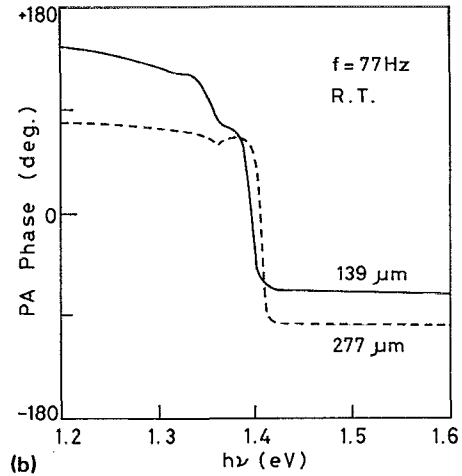
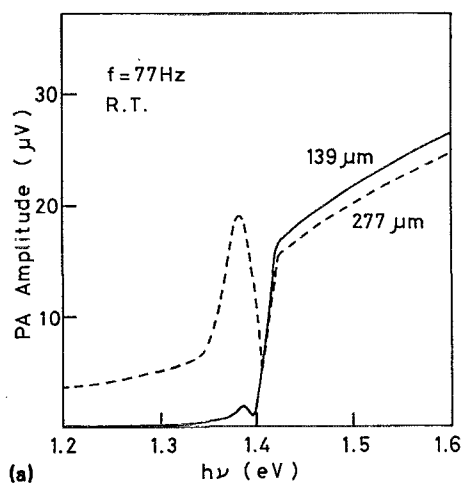


FIG. 2. (a) The PA amplitude and (b) the phase spectra for thin samples of 277  $\mu\text{m}$  (dashed) and 139  $\mu\text{m}$  (solid curve).  $f$  was set at 77 Hz.

2(b)] is almost the same as that for the sample of  $L = 530 \mu\text{m}$  in Fig. 1. However, the height of the A peak relative to that of the higher-energy region above  $E_g$  decreases. For the thinnest sample of  $L = 139 \mu\text{m}$ , the A peak becomes significantly small. The peak energy slightly shifts to the higher-energy side for the thinner samples. The difference of the A-peak energy is about 5 meV between 530- and 139- $\mu\text{m}$ -thick samples. A pronounced decrease of the phase signal appears for the 139- $\mu\text{m}$ -thick sample near 1.36 eV as shown in Fig. 2(b). This decrease of the phase corresponds to the observed dip near 1.36 eV in the phase spectra of Fig. 1(b).

In the case for the spectra of Figs. 1 and 2, the PZT detector was attached to the rear side of the sample surface with respect to the incident light beam. Since the detector geometry drastically influences the PA spectral shapes,<sup>2</sup> the PA measurements were also carried out by using a ring-shaped PZT transducer attached to the front surface of the sample. The light beam was directed to the sample surface through the annulus of the detector, and the detector itself was shaded from the incident light. The results are shown in Fig. 3. The observed PA signal is of the order of a few microvolts which is about ten times smaller than

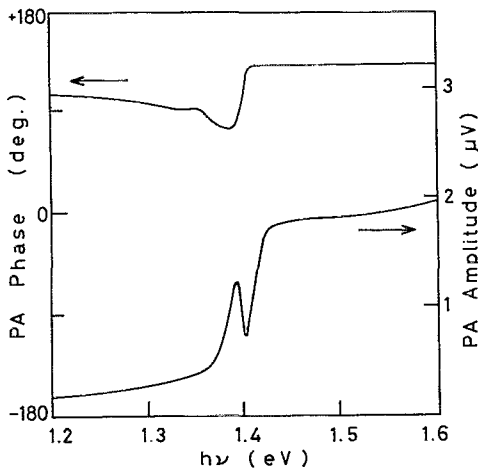


FIG. 3. The PA amplitude and the phase spectra when the detector was attached to the front surface of the sample, where  $L = 550 \mu\text{m}$  and  $f = 77 \text{ Hz}$ .

that in Figs. 1(a) and 2(a). The peak in the amplitude spectra is also observed in this detector geometry: The peak is observed at 1.392 eV and is slightly shifted to the higher  $h\nu$  region. The phase advances about  $+40^\circ$  across  $E_g$  contrary to that in Figs. 1(b) and 2(b), where the phase is always delayed about  $180^\circ$ .

### III. DISCUSSION AND CONCLUSION

As shown in the PA amplitude spectra in Figs. 1(a), 2(a), and 3, the PA signal in the lower-energy region below about 1.35 eV monotonously increases with  $h\nu$  and merges into the tail of the A peak. The similar continuous absorption band below  $E_g$  has also been observed for the SI LEC-grown GaAs by ir-absorption measurements at 9 K by Fischer,<sup>8</sup> who concluded that this absorption is due to the EL2 deep levels. Since the absorption coefficient  $\beta$  due to the EL2 defects is expected to be lower than  $10 \text{ cm}^{-1}$ , the product  $\beta L$  becomes 0.5 when the sample thickness is about  $500 \mu\text{m}$ . This is in the region where the linear dependence of the PA signal on  $\beta$  would be expected.<sup>2</sup> This means that the observed signal in the PA spectra below the A-peak reflects directly the absorption spectra. Therefore, we conclude that the broad band below 1.35 eV in the PA amplitude spectra is due to the transitions involving the EL2 centers. It should be emphasized here that the low density of EL2 could be observed for the thin samples less than  $500 \mu\text{m}$  using PA measurements. Usual transmittance measurements require a sample a few mm thick to detect such low levels of the absorption coefficient and such thick samples are difficult to prepare. A detailed discussion, especially in the lower- $h\nu$  region below 1.2 eV, will be provided elsewhere.

We have already reported the PA amplitude spectra of SI GaAs and have assigned the observed peak at 1.38 eV to the transitions concerned with the dislocations.<sup>6</sup> However, an alternative explanation of the A peak still seems to be possible. When the heat is generated in the solid samples by the nonradiative deexcitation process, the thermal and

elastic waves propagate through the sample. The piezoelectric PA technique is intended to detect these waves simultaneously. Since the disk-shaped PZT detector is attached to the rear side of the sample in our experiments,<sup>6</sup> there is a possibility that an apparent maximum appears in the PA spectra.<sup>2</sup> We discuss this possibility in detail to investigate the PA signal generation mechanism.

The theory of a piezoelectric PA spectroscopy has been developed by Jackson and Amer.<sup>2</sup> When the light is incident on the center of the platelet sample, the temperature of the illuminated volume increases and leads to an expansion of that region as well as an outflow of heat. In the case of a weakly absorbing solid, the incident light is transmitted through the sample and the heat is generated in the entire region of the sample. The enlargement of the central illuminated region causes the general expansion of both the front and the rear surface of the sample. In the case of strongly absorbing solids, however, the light beam is completely absorbed in the illuminated thin surface layer. Then, the heat generated in this region decays spatially along the thickness of the sample. Consequently, the front position of the sample expands more than the rear, resulting in a bending of the sample. Such bending compresses the rear surface and opposes the general expansion. Therefore, when the PA spectra are measured near the optical-absorption edge, the PA spectral shape should be strongly affected by the detector geometries.

Assuming that the pyroelectric effect is negligible and the sample is thick compared to the PZT transducer and the transducer is relatively compliant, the observed PA voltage by the detector is given by<sup>2</sup>

$$V \sim \beta \{ -r \exp(-KL)F(KL) - r \exp(KL)F(-KL) + r \exp(-\beta L)F(KL) + r \exp(-\beta L)F(-KL) - \exp(-KL)F(-\beta L) + \exp(KL)F(-\beta L) \} \times \{ (\beta^2 - K^2) [\exp(-KL) - \exp(KL)] \}^{-1}, \quad (1)$$

where

$$F(m) = [\exp(m) - 1] / m \pm 6 [(1 + m/2) - \exp(m)(1 - m/2)] / m^2. \quad (2)$$

The plus sign is valid when the detector is away from the incident beam, i.e., the detector is attached on the rear side of the sample. When the detector is on the front side of the sample, one should use the negative sign. The surface conduction from the sample to the surroundings was supposed to be negligible. In Eq. (1),  $K^2 = i\omega/\lambda$  and  $r = \beta/K$ , where  $\lambda$  is the thermal diffusivity,  $\omega = 2\pi f$  and  $i^2 = -1$ . The thermal diffusivity  $\lambda$  is defined by  $\kappa/\rho C$ , where  $\rho$  is the density,  $\kappa$  the thermal conductivity and  $C$  the specific heat. In the present case of GaAs, we use the parameters  $\rho = 5.32 \text{ g/cm}^3$ ,  $\kappa = 0.46 \text{ W/cm K}$ , and  $C = 0.35 \text{ J/g K}$  for the calculation.

By using Eq. (1) and the physical parameters for GaAs, the expected PA spectrum as a function of the optical-absorption coefficient  $\beta$  is easily calculated. However, the PA signal as a function of the incident photon energy

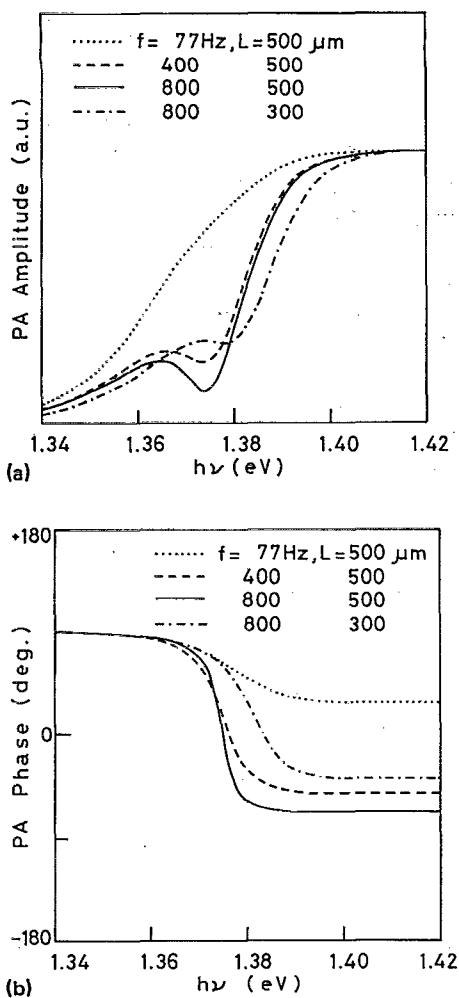


FIG. 4. (a) The calculated PA amplitude and (b) phase spectra by using Eq. (1): dotted curves for  $f = 77$  Hz and  $L = 500 \mu\text{m}$ ; dashed curves for 400 Hz and  $500 \mu\text{m}$ ; solid curves for 800 Hz and  $500 \mu\text{m}$ ; and dot-dashed curves for 800 Hz and  $300 \mu\text{m}$ .

$h\nu$  would be preferable for comparing the present model with the experimental results. The absorption spectra near the energy gap  $E_g$  of GaAs has been reported by Moss and Hawkins.<sup>9</sup> Their results are reproduced in Fig. 1(a) by the thin dot-dashed curve. The  $\beta$  at  $E_g$  is of the order of  $10^3 \text{ cm}^{-1}$ . Below the energy gap,  $\beta$  vs  $h\nu$  is well interpreted by the exponential behavior (so-called Urbach's tail) down to  $\beta$  around  $2 \text{ cm}^{-1}$ . Therefore, the expected PA spectrum as a function of  $h\nu$  was deduced by using Eq. (1) and supposing that  $\log \beta$  is proportional to  $h\nu$ . The parameters of the Urbach's tail were evaluated to obtain a best fit to the absorption spectra<sup>9</sup> below  $E_g$  in Fig. 1(a).

We have calculated the expected PA signal versus  $h\nu$  by changing the modulation frequency  $f$  and the sample thickness  $L$  from 77 to 800 Hz and from 100 to  $500 \mu\text{m}$ , respectively. Typical calculated PA amplitude and the phase spectra as a function of  $h\nu$  are shown in Figs. 4(a) and 4(b), respectively. The PZT detector was supposed to be at the rear side of the sample. The amplitude spectra were normalized at high values of  $\beta$  above  $E_g$ . The PA amplitude signal for  $f = 77$  Hz and  $L = 500 \mu\text{m}$  is directly

proportional to  $\beta$  for the small value of  $\beta$  and is saturated for the higher values of  $\beta$ . No maximum appears. The phase delays from  $+90$  to  $+30^\circ$  with the increase of  $\beta$  across  $E_g$ . For the spectra of  $f = 800$  Hz and  $L = 500 \mu\text{m}$ , a distinctive maximum and dip occurs at 1.365 and 1.375 eV, respectively. Hereafter we refer to this maximum as an apparent maximum. The appearance of the maximum and the dip is caused by the bending of the sample when the  $\beta$  increases as discussed qualitatively above. The incident light is completely absorbed in thin surface layer of the sample. The energies  $h\nu$  at the maxima and the dips in the calculated PA amplitude spectra do not change drastically with a change in  $f$ . However, a small but finite change of the energy of the maximum is observed by changing the sample thicknesses  $L$  and is estimated graphically from the calculated curves. Although the height of the maximum relative to that above  $E_g$  almost remains constant, the depth of the dip becomes deeper when  $f$  and  $L$  increases. The phase changes near the apparent maxima become more steep when  $f$  and  $L$  increase.

In the experimentally observed PA amplitude spectra in Fig. 1(a) for  $L = 530 \mu\text{m}$  and  $f = 77$  Hz, the large A peak at 1.383 eV was observed. Since no maximum appears in the calculated spectra for these  $f$  and  $L$ , the presence of the A peak in the experimental results is curious. However, we suppose here conventionally that the A peak always appears even for low  $f$  and small  $L$  in order to discuss the shifts of the observed peaks and dips. Accordingly the appearances of the A peak in Figs. 1(a) and 2(a) can be expected in the calculated curves, even when the optical-absorption coefficient  $\beta$  monotonously increases with  $h\nu$ . The sudden decrease of the signal phase with increase of  $h\nu$  near the dip in the amplitude spectra is also expected. The energy of the A peak in Fig. 1(a) is almost unchanged with  $f$  within our experimental error and this fact agrees with the calculated curves in Fig. 4(a). The phase change in Fig. 1(b) is also well interpreted by the present model calculation. However, one significant disagreement between the model and the experimental results remains. This is for the frequency dependence of the heights of the A peak. They are larger than that above  $E_g$  at low  $f$  and become smaller when  $f$  increases from 77 to 800 Hz as shown in Fig. 1(a). This variation of the peak height with  $f$  could not be interpreted by the present model using Eq. (1). Details are discussed below.

The effect of the sample thicknesses  $L$  on the PA amplitude and the phase spectra were also calculated. The results show that the energies of the maxima and the dips shift toward the lower-energy region when the sample thickness  $L$  increases. From the graphical analysis of different  $L$  as shown in Fig. 4, the energy shift of the A peak can be estimated as 0.015 eV between 530- and 139- $\mu\text{m}$ -thick samples. The height of these apparent maxima do not change drastically with  $L$  and the PA amplitude signals always saturate in the higher value of  $\beta$ . In the experimental results in Figs. 1(a) and 2(a), the A peak appears at 1.383, 1.384, and 1.388 eV for 530-, 277-, and 139- $\mu\text{m}$ -thick samples, respectively. Since our observed shift of 0.005 eV is considerably smaller than the expected value,

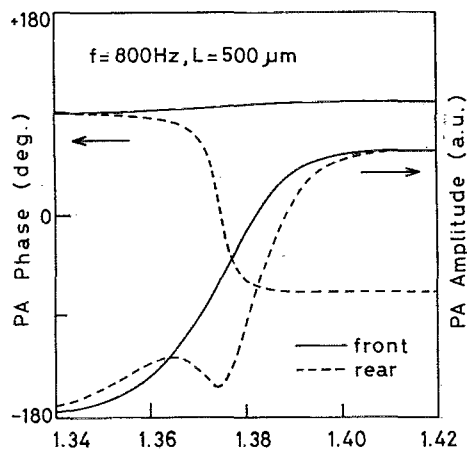


FIG. 5. The calculated PA amplitude and the phase spectra, where the detector is at the front side of the sample (solid curves):  $L = 500 \mu\text{m}$  and  $f = 800 \text{ Hz}$ . The calculated spectra for the rear surface detector are also shown by the dashed curve to aid in comparison.

the peak shift with the sample thickness could not be well explained by the present model.

We consider here again the variations of the height of the A peak with  $f$  and  $L$ . One of the critical assumptions in deriving Eq. (1) is that the pyroelectric effect was not taken into account. This effect may also be important in understanding the peak height variations. In the case where only the generated heat caused by the absorption of light was detected directly by the transducer at the rear side of the sample, we can alternatively apply the Rosenzweig and Gersho model<sup>10</sup> to explain the experimental results. The results of the calculations show that the apparent maximum can also be expected for high values of  $L$  and  $f$  as in the case of Jackson and Amer's model. The peak height increases with increases of  $L$  and  $f$ . Although the increase in peak heights with the increase of  $L$  can be expected from this alternative model, their  $f$  dependence still disagrees with the experimental results. The peak heights become smaller with  $f$  in our observed results.

The PA amplitude and the phase spectra of different detector geometry, where the piezoelectric transducer is at the sample front surface toward the incident light, are calculated by using Eq. (1) and the results are shown in Fig. 5. The typical case of  $f = 800 \text{ Hz}$  and  $L = 500 \mu\text{m}$  is drawn in the figure. The calculated spectra for the back-surface detector geometry were also shown in the figure by the dashed curve to aid in comparison. When the detector is at the front surface of the samples, the calculated spectra show that the PA signal amplitude monotonously increases and saturates with the increases of  $h\nu$ . No apparent maximum appears. The phase slightly advances with the increase of  $h\nu$  and the phase shift is about  $+10^\circ$ . However, in the experimental results as shown in Fig. 3, a distinctive peak evidently appeared at 1.392 eV and the phase delayed prior to the advance above 1.40 eV. According to the calculated curves by using Eq. (1), no such peak and no delay of the phase are expected. If this peak is supposed to be an apparent maximum as in the case when the detector was at

the rear side of the sample, the complex signal generation mechanism should be necessary to interpret the origin of this peak.

From the discussions above, it is concluded that the observed A peak in the PA spectra could not be interpreted by any of the proposed models for the PA signal generation mechanisms. This suggests that the A peak is not an apparent maximum but has a physical origin. In the previous report on the PA spectra of SI GaAs,<sup>6</sup> we suggested that the peak height increases with the etch pit densities (EPD) of the samples, which may be proportional to the dislocation densities. Although we have never carried out PA measurements for samples with different EPDs in a wide range of variety, the dislocations in the crystal may play an important role in PA signal generation.

In the previous report, we also showed the PA spectra measured at low temperatures, at 181 and 91 K.<sup>6</sup> When the samples were cooled down, the height of the A peak increased drastically compared with the signals far above  $E_g$  in the experimental results. We have also tried to calculate the expected PA spectra at low temperature by using Eq. (1) to investigate the variation of the spectral shape with temperature. The temperature dependence of the absorption coefficient is included in the experimental factor of the Urbach's tail discussed above. The slope of  $\log \beta$  vs  $h\nu$  becomes steeper when the temperature decreases.<sup>11</sup> We have calculated the PA spectra by using the exponential dependencies of the absorption spectra and Eq. (1), and we have found that the calculated height of the apparent maxima never change with a decrease in temperature down to about 5 K. This is contrary to our experimental results: The observed height of the A peak drastically changed with the temperatures. Thus, the proposed model cannot explain the results. If the A peak has a physical origin, e.g., due to the localized electronic states in the energy band gap, the thermally activated behavior of the peak height can be expected, and the peak height may drastically change with temperature as in the case observed in the experimental results.

Another indication that the A peak is not an apparent one can be seen in our previous report of the PA spectra for layer semiconductors InSe, GaSe,<sup>1</sup> and BiI<sub>3</sub>,<sup>3</sup> which have absorption coefficients from  $10^3$  to  $10^5 \text{ cm}^{-1}$  at the exciton peaks. No peak has ever been observed in the room-temperature PA spectra. The PA signal monotonously increase with  $h\nu$  and saturates far above  $E_g$ . Since GaAs has a  $\beta$  of the order of  $10^3 \text{ cm}^{-1}$  just above  $E_g$ , a similar spectrum as that for the layer semiconductors may be expected; no apparent maximum will be seen.

In conclusion, we have obtained the PA amplitude and the phase spectra of *n*-GaAs by changing the modulation frequencies  $f$  and sample thicknesses  $L$ . We concluded that the observed broad band below 1.35 eV in the PA spectra is due to the electron transitions involving the EL2 deep-defect levels by comparing with the optical-absorption spectra. As for the A peak at 1.383 eV in the PA amplitude spectra, we have done some model calculations as proposed by Jackson and Amer, where the piezoelectric detector is attached to the rear side of the sample. Although

the observed shift of the A-peak energy by changing the sample thickness  $L$  has the same sign as that estimated from Eq. (1), their values are quite different, and the variation of the A-peak height with  $f$  and  $L$  exhibits an opposite tendency between the experimental results and the theoretically expected curves. Accordingly, we consider at the present time that the A peak is not an apparent one but has a physical origin. Further investigations are now proceeding to understand what gives rise to the A peak in the PA spectra of GaAs.

<sup>1</sup>T. Ikari, S. Shigetomi, and Y. Koga, in *Photoacoustic and Thermal Wave Phenomena in Semiconductors*, edited by A. Mandelis (Elsevier, New York, 1987), p. 397.

- <sup>2</sup>W. Jackson and N. M. Amer, *J. Appl. Phys.* **51**, 3343 (1980).  
<sup>3</sup>T. Ikari, S. Shigetomi, H. Nishimura, H. Yayama, and A. Tomokiyo, *Phys. Rev. B* **37**, 886 (1988).  
<sup>4</sup>K. Wasa, K. Tsubouti, and N. Mikoshiba, *Jpn. J. Appl. Phys.* **19**, L475, and L653 (1980).  
<sup>5</sup>G. P. Caesar, H. Abkowitz, and J. W. P. Lin, *Phys. Rev. B* **29**, 2353 (1984).  
<sup>6</sup>T. Ikari, H. Yokoyama, K. Maeda, and K. Futagami, *Phys. Status Solidi A* **121**, K125 (1990).  
<sup>7</sup>T. Ikari, H. Yokoyama, S. Shigetomi, and K. Futagami, *Jpn. J. Appl. Phys.* **29**, 887 (1990).  
<sup>8</sup>D. W. Fischer, *Appl. Phys. Lett.* **50**, 1751 (1987).  
<sup>9</sup>T. S. Moss and T. D. F. Hawkins, *Infrared Phys.* **1**, 111 (1961).  
<sup>10</sup>A. Rosencwaig and A. Gersho, *J. Appl. Phys.* **47**, 64 (1976).  
<sup>11</sup>D. Redfield and M. A. Afromowitz, *Appl. Phys. Lett.* **11**, 138 (1967).

Journal of Applied Physics is copyrighted by the American Institute of Physics (AIP). Redistribution of journal material is subject to the AIP online journal license and/or AIP copyright. For more information, see <http://ojps.aip.org/japo/japcr/jsp>  
Copyright of Journal of Applied Physics is the property of American Institute of Physics and its content may not be copied or emailed to multiple sites or posted to a listserv without the copyright holder's express written permission. However, users may print, download, or email articles for individual use.